

Bose-Einstein Condensation in Multilayers

P. Salas · M. Fortes · M. de Llano · F.J. Sevilla ·
M.A. Solís

Received: 12 January 2010 / Accepted: 24 February 2010
© Springer Science+Business Media, LLC 2010

Abstract The critical BEC temperature T_c of a non interacting boson gas in a layered structure like those of cuprate superconductors is shown to have a minimum $T_{c,m}$, at a characteristic separation between planes a_m . It is shown that for $a < a_m$, T_c increases monotonically back up to the ideal Bose gas T_0 suggesting that a reduction in the separation between planes, as happens when one increases the pressure in a cuprate, leads to an increase in the critical temperature. For finite plane separation and penetrability the specific heat as a function of temperature shows two novel crests connected by a valley in addition to the well-known BEC peak at T_c associated with the 3D behavior of the gas. For completely impenetrable planes the model reduces to

P. Salas

Posgrado en Ciencia e Ingeniería de Materiales, Universidad Nacional Autónoma de México,
Apdo. Postal 70-360, 04510 México, DF, Mexico
e-mail: patysalasc@hotmail.com

M. Fortes · F.J. Sevilla · M.A. Solís (✉)

Instituto de Física, Universidad Nacional Autónoma de México, Apdo. Postal 20-364,
01000 México, DF, Mexico
e-mail: masolis@fisica.unam.mx

M. Fortes

e-mail: fortes@fisica.unam.mx

F.J. Sevilla

e-mail: fjsevilla@fisica.unam.mx

M. de Llano

Physics Department, University of Connecticut, Storrs, CT 06269, USA
e-mail: dellano@servidor.unam.mx

M. de Llano

Instituto de Investigaciones en Materiales, Universidad Nacional Autónoma de México,
Apdo. Postal 70-360, 04510 México, DF, Mexico

many disconnected infinite slabs for which just one hump survives becoming a peak only when the slab widths are infinite.

Keywords Bose-Einstein condensation · Multilayers · Critical temperature · Specific heat

1 Introduction

Bose-Einstein condensation in a layered system has been studied almost since London suggested [1, 2] that superfluidity could be an expression of Bose-Einstein condensation (BEC) of atoms in liquid helium, to understand helium films [3–6]. The discovery of high temperature superconductivity stimulated a renewed interest in systems with layered structures [7, 8] in which a BEC mechanism may play a part in the determination of the critical temperatures [9]. In fact, it has been pointed out [10–13] that the BEC concept is of fundamental importance to understand cuprate superconductivity. In addition, recent experimental results on Bose-Einstein condensates [14, 15] or superfluidity of ultracold fermions [16] in optical lattices, and the expectation to obtain BEC of excitons in semiconductors [17, 18], have revived theoretical and experimental [19, 20] efforts to understand the behavior of quantum gases in a periodical or non-periodical [21, 22] structure.

Most models based on layered structures [9, 23–26] simulating quasi-2D high- T_c superconductors, or other to study BEC [27–29], rely on a single-boson hopping interaction term producing nearest-interlayer couplings in one spatial dimension while moving freely in the other two directions. The energy spectrum is typically of the form $\epsilon_{\mathbf{k}} = \hbar^2(k_x^2 + k_y^2)/2m + \epsilon_{k_z}$ with $\epsilon_{k_z} = (\hbar^2/Ma^2)(1 - \cos k_z a)$ where a is the plane separation and the constant \hbar^2/Ma^2 is a measure of the bosonic Cooper pair hopping probability between planes. In the case of CuO_2 planes in cuprate superconductors, the boson effective mass M in the z -direction accounts for the cuprate anisotropy by requiring $M \gg m$ where m is the mass in the x -, y -directions. For $k_z a \ll 1$ the expected result $\epsilon_{k_z} = \hbar^2 k_z^2 / 2M$ is recovered. However, a more realistic model should include the motion of bosons in a truly 3D scenario where the bosons are moving, not hopping between layers, particularly when the true, moderate values of the interlayer separation, a , are considered.

Motivated by future applications to quasi-2D superconductors or to ^4He films, in this work we discuss critical temperature T_c and the specific heat C_V results in a non-interacting boson gas of N particles within an infinite multilayered structure of equally-spaced planes of variable penetrability stacked in the z -direction.

In the next section we describe our system and derive the particle energy as a function of its momentum. In Sect. 3 we calculate the critical temperature and specific heat as a function of plane separation and impenetrability. Section 4 contains our conclusions.

2 Boson Among Plane Layers

The system of parallel planes is described by a 1D periodic delta potential of the Kronig-Penney (KP) type along the z -direction while bosons move freely in the two

remaining directions. Two important differences with previous studies [9, 27–29] are: (a) in our model the bosons are allowed to move over all space through permeable planes instead of constraining them to move only over the plane surfaces, and (b) the anisotropy expected from a layered material is introduced naturally by the delta KP potential. In addition, the delta strengths avoid the introduction of large masses and hopping parameters in the z -direction to tune the mobility or tunneling across planes. At very low energies the KP potential reduces to the energy expression ϵ_{k_z} used in Refs. [9, 27–29] which only takes into account the lowest allowed energy band. If T_0 is the critical BEC temperature of the free 3D boson gas and the associated thermal wavelength is $\lambda_0 \equiv h/\sqrt{2\pi mk_B T_0}$ a dimensionless “impenetrability” $P_0 \equiv P\lambda_0 \geq 0$ of layers is introduced in terms of the KP penetrability parameter P [see (1) below]. Thus, $P_0 = 0$ implies perfect layer transparency and $P_0 = \infty$ fully opaque layers. In the latter limit, our model reduces to that of an infinite number of uncoupled slabs of thickness a and infinite lateral extent. The specific heat has been obtained in these slabs to model ^4He thin-film properties [30–35] and finite-size effects on BEC [36]. In these infinite slabs the BEC critical temperature is zero but the specific heat shows a smooth maximum at a temperature that depends on the slab thickness. Some authors [33–36] have associated this “hump” with a BEC signature. However, we will show that for finite P_0 this hump coexists with a nonzero critical BEC temperature in addition to a second maximum. Furthermore, when $P_0 \rightarrow \infty$ the BEC temperature goes to zero whereas the hump persists to become the familiar BEC with a *cusped* sharp peak only in the limit $a/\lambda_0 \rightarrow \infty$.

The Schrödinger equation for a boson of mass m is separable in the x -, y - and z -directions so that the single-particle energy as a function of the wavevector $\mathbf{k} = (k_x, k_y, k_z)$ is simply $\epsilon_{\mathbf{k}} = \epsilon_{k_x} + \epsilon_{k_y} + \epsilon_{k_z}$, where $\epsilon_{k_x, k_y} = \hbar^2 k_{x,y}^2/2m$ with $k_{x,y} = 2\pi n_{x,y}/L$ and $n_{x,y} = 0, \pm 1, \pm 2, \dots$, i.e., in the x - and y -directions particles are free and we assume periodic boundary conditions in a box of size L . In the z -direction the particles are subject to the KP periodic delta (or “Dirac comb”) potential [37, 38] and the energies ϵ_{k_z} are implicit in the transcendental equation

$$Pa \frac{\sin \alpha a}{\alpha a} + \cos \alpha a = \cos k_z a \tag{1}$$

where $\alpha^2 \equiv 2m\epsilon_{k_z}/\hbar^2$ and $\hbar^2 P/m$ is the delta-interaction strength or equivalently, the layer impenetrability parameter. For finite P , bosons tunnel through the layers as a more realistic model would demand. The energy $\epsilon_{k_z j}$ depends on the parameters P and a where the band structure is labeled with the index $j = 1, 2, \dots$. The trivial free-particle energy dispersion relation in the z -direction, $\epsilon_{k_z j} \rightarrow \hbar^2 k_z^2/2m$, is recovered in the limit $P \rightarrow 0$, while $P \rightarrow \infty$ yields $\sin(\alpha a) \rightarrow 0$ which corresponds to a system of confined bosons inside a semi-infinite slab of width a , a situation extensively discussed in the literature (see [34, 35] and references therein). For $\alpha a \ll 1$, (1) can be expanded and rewritten as

$$\epsilon_{k_z} \simeq \frac{\hbar^2}{2ma^2} \frac{Pa + (1 - \cos k_z a)}{1/2 + Pa/6} = \frac{\hbar^2}{Ma^2} [Pa + (1 - \cos k_z a)] \tag{2}$$

where the second term in the last expression is the dispersion relation used in Refs. [9, 27, 29] with mass $M = m(1 + Pa/3)$. Therefore, the magnitude of M can be interpreted as a measure of the plane impenetrability P of this model.

3 Critical Temperature and Specific Heat

The grand potential $\Omega(T, V, \mu) = -pV$ (with p the pressure, V the volume and μ the chemical potential) leads to the thermodynamic properties. In our multilayered system it becomes, after integrating over k_x and k_y ,

$$\Omega(T, V, \mu) = \Omega_0 - \frac{1}{\beta^2} \frac{Vm}{(2\pi)^2 \hbar^2} \sum_{j=1}^{\infty} \int_{-\pi/a}^{\pi/a} dk_z g_2(ze^{-\beta\epsilon_{k_z j}}) \tag{3}$$

where $z \equiv e^{\beta\mu}$ is the fugacity, $\beta \equiv 1/k_B T$, and we have explicitly separated the contribution $\Omega_0 \equiv k_B T \ln[1 - ze^{-\beta\epsilon_0}]$ of the lowest-energy state ϵ_0 . Here $g_\sigma(t)$ stands for the Bose function [39]. The integration is over the first Brillouin zone and the sum is over the allowed bands. Note that the ground-state energy ϵ_0 depends on both P and a in (1).

3.1 Critical Temperature

The average number of particles $N = -(\partial\Omega/\partial\mu)_{T,V}$ for a free boson gas in the multilayered configuration is then

$$N = N_0(T) - \frac{Vm}{(2\pi)^2 \hbar^2} \frac{1}{\beta} \sum_{j=1}^{\infty} \int_{-\pi/a}^{\pi/a} dk_z \ln[1 - ze^{-\beta\epsilon_{k_z j}}] \tag{4}$$

where $N_0(T) \equiv [z^{-1}e^{\beta\epsilon_0} - 1]^{-1}$ is the number of particles condensed in the ground state ϵ_0 while the last term in (4) is the number of particles in excited states. As usual, the BEC critical temperature T_c is obtained by finding the temperature below which the fractional number of particles in the ground state just ceases to be negligible upon cooling and the chemical potential reaches its maximum value $\epsilon_0 > 0$ making the fugacity $z_0 = e^{\beta_c\epsilon_0}$. For convenience and clarity we use the same particle density N/V in the layered system as that for the free ideal Bose gas (IBG) with the BEC critical temperature T_0 . Thus $k_B T_0$ serves as an energy scale while $\lambda_0 \equiv h/\sqrt{2\pi mk_B T_0}$ provides a length scale.

The effects of the KP layers on BEC are shown in Fig. 1 where T_c/T_0 decreases as P_0 increases for different values of a . Note that the critical temperature is very sensitive to the number of energy bands intervening in the numerical calculations. Here, it is sufficient to include 10 bands to achieve convergence for the values of a and P_0 shown in the figure. When $P_0 = 0$ (perfect barrier transparency) we recover the IBG results. In the opposite limit $P_0 \rightarrow \infty$ (impenetrable barriers) T_c/T_0 vanishes like a system with effective dimensionality two although strictly speaking, the model does not become true 2D unless $a = 0$.

Fig. 1 Critical temperature T_c in units of T_0 as a function of P_0 for different values of a/λ_0

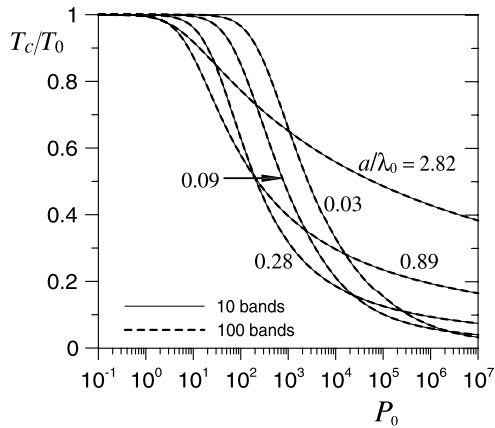
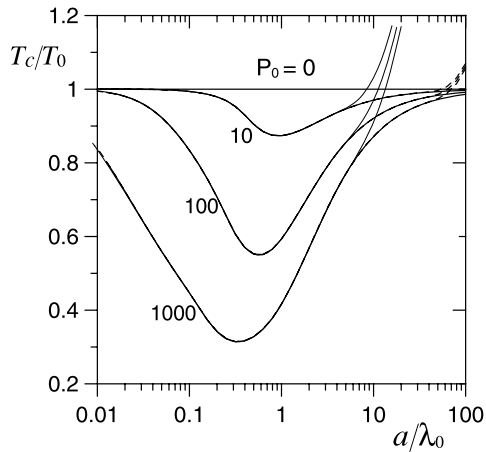


Fig. 2 Critical temperature as a function of a/λ_0 for different values of P_0 . Thin, dashed and normal lines correspond to 10, 100 and 1000 energy bands, respectively. For $a/\lambda_0 \lesssim 5$ numerical convergence is attained with 10 bands and the curves coincide. For $a/\lambda_0 \gtrsim 5$ one must consider a larger number of energy bands



A novel result shown in Fig. 2 is that for finite P_0 , T_c/T_0 diminishes from 1 down to a minimum value as the plane separation a decreases. For P_0 spanning at least five orders of magnitude (see Table 1) the critical-temperature minima show a linear dependence with a_m so that $T_{c,m} = (T_0/\lambda_0)a_m$ or $(\lambda_0/\lambda_{c,m})^2 = a_m/\lambda_0$, where the subscript m means minimum and $\lambda_{c,m}$ is the thermal wave length associated to $T_{c,m}$. Since $T_{c,m} \rightarrow 0$ and $a_m \rightarrow 0$ for $P_0 \rightarrow \infty$ this linear relation seems to hold for all $P_0 \gtrsim 10$. For $P_0 \lesssim 10$, $T_{c,m}/T_0$ approaches 1 while $a_m \rightarrow \infty$. Surprisingly, further reduction in a brings an increase in T_c/T_0 which asymptotically reaches unity. This can be understood from the KP dispersion relation (1) since for small values of a $\sin(\alpha a)/\alpha a \simeq 1$ and $\varepsilon_{k_z j} \simeq \hbar^2 k_z^2/2m$ so that one recovers the 3D IBG regime when $a \rightarrow 0$, as expected. We also note in Fig. 2 that T_c/T_0 is not symmetric with respect to the minimum value. For $a/\lambda_0 \ll 1$, T_c/T_0 increases slower than for $a/\lambda_0 \gg 1$. This asymmetry may be explained by the a -dependance of the system total density of states $g(\varepsilon)$. For values of $a \gg \lambda_0$, $g(\varepsilon)$ approaches slowly to that of the ideal 3D boson gas $\propto \varepsilon^{1/2}$. In contrast, for values of $a \ll \lambda_0$, energy gaps and band widths grow inversely with a and only the “quadratic” bottom of the first band contributes

Table 1 Values of plane separation a_m for which the critical temperature reaches its minimum for different P_0

P_0	10	10^2	10^3	10^4	10^5
a_m/λ_0	0.874	0.550	0.314	0.177	0.100
$T_{c,m}/T_0$	0.927	0.572	0.337	0.191	0.107

to the calculation of T_c . The density of states then behaves effectively as [40] $g(\tilde{\varepsilon}) \propto \tilde{\varepsilon}^{1/2}$, where $\tilde{\varepsilon}$ is the energy measured from the ground state value. We also note that for $a/\lambda_0 \gg 1$ one must include more than ten energy bands to achieve convergence in the numerical calculations.

3.2 Specific Heat

The internal energy U is given by

$$U(T) = N\varepsilon_0 + \frac{L^3 m}{(2\pi)^2 \hbar^2 \beta^2} \sum_{j=1}^{\infty} \int_{-\pi/a}^{\pi/a} dk_z \{ g_2(z e^{-\beta \varepsilon_{k_z j}}) - \beta (\varepsilon_{k_z j} - \varepsilon_0) \ln[1 - z e^{-\beta \varepsilon_{k_z j}}] \} \tag{5}$$

and the specific heat $C_V = -T [\partial^2 \Omega / \partial T^2]_{V,\mu}$ is

$$\begin{aligned} \frac{C_V}{Nk_B} = & \frac{Vm}{N(2\pi)^2 \hbar^2} \sum_{j=1}^{\infty} \int_{-\pi/a}^{\pi/a} dk_z \left\{ 2k_B T g_2(z e^{-\beta \varepsilon_{k_z j}}) \right. \\ & - \ln(1 - z e^{-\beta \varepsilon_{k_z j}}) [2 \varepsilon_{k_z j} - \mu - \varepsilon_0 + T \partial \mu / \partial T] \\ & \left. + \frac{1}{k_B T} \frac{(\varepsilon_{k_z j} - \varepsilon_0) [\varepsilon_{k_z j} - \mu + T \partial \mu / \partial T]}{z^{-1} e^{\beta \varepsilon_{k_z j}} - 1} \right\} \tag{6} \end{aligned}$$

where

$$T(\partial \mu / \partial T) = \frac{-\frac{N}{V} \frac{(2\pi)^2 \hbar^2}{m} - \sum_{j=1}^{\infty} \int_{-\pi/a}^{\pi/a} dk_z \frac{\varepsilon_{k_z j} - \mu}{z^{-1} e^{\beta \varepsilon_{k_z j}} - 1}}{\sum_{j=1}^{\infty} \int_{-\pi/a}^{\pi/a} dk_z [z^{-1} e^{\beta \varepsilon_{k_z j}} - 1]^{-1}} \tag{7}$$

For $T < T_c$ the chemical potential $\mu = \varepsilon_0$ is a constant so that $\partial \mu / \partial T = 0$ which simplifies the equation for C_V / Nk_B . Numerical results are summarized in Fig. 3 of C_V / Nk_B vs. $\log T / T_0$ and vs. $\log a / \lambda_0$ for an intermediate dimensionless penetrability $P_0 = 100$. In contrast with the IBG case, in addition to the familiar BEC peak for finite P_0 two humps appear that are connected by a valley when $T > T_c$; the hump heights depend on the plane separation. When $a > a_m$ only one hump survives and becomes the BEC cusped peak in the limit $a \rightarrow \infty$ independently of P_0 . Our model shows the distinct nature of the ever present BEC critical temperature plus a *second* characteristic temperature where C_V / Nk_B is maximum. In previous models (here

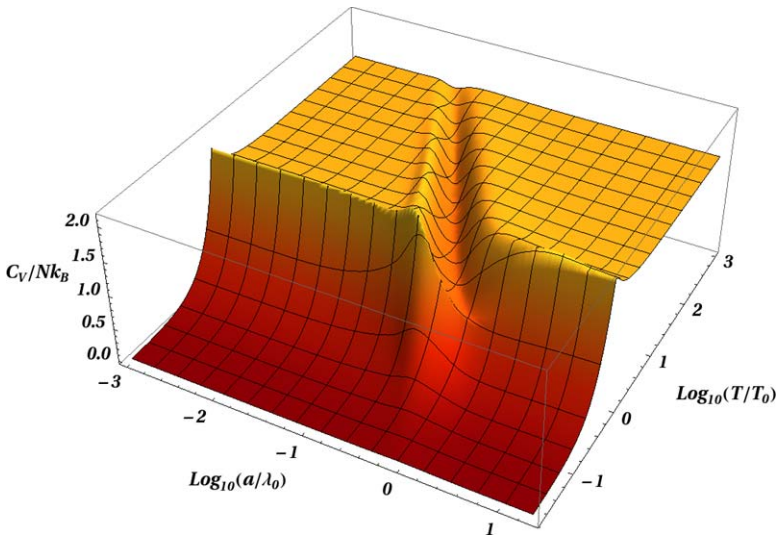
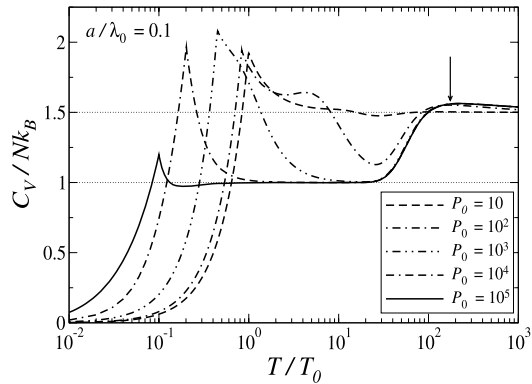


Fig. 3 (Color online) 3D plot of the specific heat as function of temperature and plane separation a for $P_0 = 100$

equivalent to $P_0 \rightarrow \infty$) [34–36] this latter temperature is identified as a signature of the BEC critical temperature. However, our results indicate that this characteristic temperature should be associated with a different feature, namely an accumulation of bosons in the lowest energy levels [41].

While C_V/Nk_B of the IBG decreases monotonically for $T > T_c \equiv T_0$, in the present model there is a region defined by $a \lesssim a_m$ where C_V/Nk_B varies non-monotonically with T having a set of local minima (the valley in Fig. 3). We found that the thermal wavelengths associated to those temperatures along the valley satisfy $\lambda \simeq 2a$. From this last relation we may conclude that the single-particle (thermal) average wavefunction nodes, coincide with the plane locations resulting in the particle motion freezing out in the z -direction. In particular, for $a = a_m$ the minimum of $C_V(T)/Nk_B$ attains its lowest value $\simeq 1$ so that the “valley” reveals a closer resemblance to a 2D system. As P_0 increases, this 2D-like feature dominates as the valley levels out over a broader temperature region (see Fig. 4 for $a/\lambda_0 = 0.1$). In addition, for temperatures below T_c the value $\lambda \simeq 2a$ marks a functional crossover of specific heat from the standard 3D IBG $C_V \propto T^{3/2}$ to the 2D linear $C_V \propto T$ behavior. For sufficiently high temperatures, layer effects are negligible regardless of penetrability P_0 as $C_V(T)/Nk_B$ approaches the 3D IBG behavior beyond the temperatures associated with the farthest maxima in Fig. 4. For $P_0 \geq 1000$ the C_V maxima are at essentially the same temperature or, equivalently, the same λ . Therefore, we can identify an a -dependent correlation length that manifests itself when $\lambda \simeq 0.7a$ as marked by the arrow in Fig. 4 for $a/\lambda_0 = 0.1$ and $T/T_0 \simeq 220$.

Fig. 4 Specific heat per particle as a function of temperature for several P_0 and $a/\lambda_0 = 0.1$. The two-dimensional character of the layered structure is easily seen as P_0 increases. The arrow indicates the initiation of the IBG regime



4 Conclusion

To conclude, we have shown that the BEC-like critical temperature as well as the specific heat of a boson gas between penetrable and periodically-spaced planes change drastically when compared to previous models based on hopping, Hubbard [9] or slab [34, 35] configurations, or when there is no confining geometrical structure whatsoever. Even though analytical approximations for the boson dispersion relation at low energies commonly used to describe layered systems have proved to be a useful guide to give more accurate results, they are significantly improved when the more accurate dispersion relation including more than one energy band is used. The appearance of two characteristic temperatures associated with the maxima of $C_V(T)$ in addition to the BEC transition temperature is shown to be a result of the plane confinement. On the other hand, this model could explain the variation of T_c with pressure in some high- T_c cuprate [42] or heavy-fermion superconductors [43] due to the structural change in the lattice parameter associated to the plane separation discussed here if the superconducting transition is related with a BEC-like phenomenon. In the limit $P_0 \rightarrow \infty$ (opaque or perfectly-decoupled infinite slabs of width a) the BEC-like transition temperature vanishes leaving only one maximum which becomes the usual cusped-peak BEC transition only when $a \gg \lambda_0$.

Acknowledgements We acknowledge partial support from grants PAPIIT IN114708 and IN106908. F.J.S. acknowledges partial support from Conacyt-SNI-I-89774. We thank O.A. Rodríguez for assistance in preparing Fig. 3.

References

1. F. London, *Nature* **141**, 643 (1938)
2. F. London, *Phys. Rev.* **54**, 947 (1938)
3. D.F. Brewer, K. Mendelssohn, *Phil. Mag.* **44**, 340 (1953)
4. S. Mehta, F.M. Gasparini, *Phys. Rev. Lett.* **78**, 2596 (1997)
5. Y. Kinoshita et al., *J. Low Temp. Phys.* **158**, 275 (2010)
6. T. Matsushita, R. Toda, M. Hieda, N. Wada, *J. Low Temp. Phys.* **150**, 032055 (2009)
7. G. Logvenov, A. Gozar, I. Bozovic, *Science* **326**, 699 (2009)
8. T. Zhang et al., *Nature Phys.* **6**, 104 (2010)

9. X.G. Wen, R. Kan, Phys. Rev. B **37**, 595 (1988)
10. Y.J. Uemura et al., Phys. Rev. Lett. **62**, 2317 (1989)
11. Y.J. Uemura et al., Phys. Rev. Lett. **66**, 2665 (1991)
12. Y.J. Uemura, J. Phys., Condens. Matter **16**, S4515 (2004)
13. Y.J. Uemura, Physica B **374–375**, 1 (2006)
14. M. Greiner, O. Mandel, T. Esslinger, T.W. Hänsch, I. Bloch, Nature **415**, 39 (2002)
15. R. Ramakumar, A.N. Das, Phys. Lett. A **348**, 304 (2006)
16. J.K. Chin et al., Nature **443**, 961 (2006)
17. J. Kasprzak et al., Nature **443**, 409 (2006)
18. L.V. Butov, J. Phys., Condens. Matter **19**, 295202 (2007)
19. P. Cladé, C. Ryu, A. Ramanathan, K. Helmerson, W.D. Phillips, Phys. Rev. Lett. **102**, 170401 (2009)
20. G. Roati et al., Nature **453**, 875 (2008)
21. X. Deng, R. Citro, E. Orignac, A. Minguzzi, Eur. Phys. J. B **68**, 435 (2009)
22. L. Sanchez-Palencia, M. Lewenstein, Nature Phys. **6**, 87 (2010)
23. R. Friedberg, T.D. Lee, Phys. Rev. B **40**, 6745 (1989)
24. R. Friedberg, T.D. Lee, H.-C. Ren, Phys. Rev. B **42**, 4122 (1990)
25. R. Friedberg, T.D. Lee, H.-C. Ren, Phys. Lett. A **152**, 417 (1991) (see also page 423)
26. R. Friedberg, T.D. Lee, H.-C. Ren, Phys. Rev. B **45**, 10732 (1992)
27. A. Hærdig, F. Ravndal, Eur. J. Phys. **14**, 171 (1993)
28. I. Trifea, I. Grosu, J. Supercond. Nov. Mag. **14**, 563 (2001)
29. T.M. Hong, J.H. Lin, Phys. Rev. B **52**, 7898 (1995)
30. J.M. Ziman, Phil. Mag. **44**, 548 (1953)
31. D.F. Goble, L.E. Trainor, Phys. Rev. **157**, 167 (1967)
32. D.F. Goble, L.E.H. Trainor, Can. J. Phys. **46**, 1867 (1968)
33. R.K. Pathria, Phys. Rev. A **5**, 1451 (1972)
34. S. Greenspoon, R.K. Pathria, Phys. Rev. A **8**, 2657 (1973)
35. S. Greenspoon, R.K. Pathria, Phys. Rev. A **9**, 2103 (1974)
36. H.R. Pajkowski, R.K. Pathria, J. Phys. A, Math. Gen. **10**, 561 (1977)
37. R. de L. Kronig, W.G. Penney, Proc. R. Soc. (Lond.) A **130**, 499 (1930)
38. D.A. McQuarrie, Chem. Educator **1**, 1 (1996)
39. R.K. Pathria, *Statistical Mechanics*, 2nd edn. (Pergamon, Oxford, 1996)
40. Details will be presented elsewhere
41. M.F.M. Osborne, Phys. Rev. **76**, 396 (1949)
42. M. Isobe, T. Ohta et al., Phys. Rev. B **57**, 613 (1998)
43. M.B. Maple, E.D. Bauer, V.S. Zapf, J. Wosnitzer, Unconventional superconductivity in novel materials, in *Superconductivity, Conventional and Unconventional Superconductors*, ed. by K.H. Benneman, J.B. Ketterson (eds.), vol. 1 (Springer, Berlin, 2008), p. 639